Removal of Arsenic from Aqueous Solutions by an Adsorption Process with Titania–Silica Binary Oxide Nanoparticle Loaded Polyacrylonitrile Polymer

A. Nilchi,[1] S. Rasouli Garmarodi,[1] S. Janitabar Darzi[1,2]

[1]*Nuclear Science and Technology Research Institute, P. O. Box 11365/8486, Tehran, Iran*
[2]*Department of Chemistry, Faculty of Sciences, Tarbiat Modares University, Tehran, Iran*

Received 30 January 2010; accepted 24 June 2010
DOI 10.1002/app.33003
Published online 29 September 2010 in Wiley Online Library (wileyonlinelibrary.com).

ABSTRACT: In this study, we fabricated a new hybrid adsorbent, titania–silica binary oxide (TiO_2–SiO_2)–polyacrylonitrile (PAN), by loading nanosized sol–gel-derived TiO_2–SiO_2 onto a porous PAN polymer for enhanced arsenite [As(III)] and arsenate [As(V)] species removal from aqueous media. The resulting sorbent was characterized by thermogravimetric analysis, scanning electron microscopy, X-ray powder diffraction, IR spectroscopy, and porosity measurements. The sorption process for the removal of As(V) and As(III) was assessed with various parameters, including the effects of the pH, contact time, temperature, and existence of foreign competing ions. We found that the adsorption of As(III) and As(V) species onto TiO_2–SiO_2–PAN was dependent on the pH of solution, and it could be well represented by the Langmuir and Dubinin–Radushkevich isotherm models. The prepared hybrid adsorbent exhibited highly selective arsenic retention from water in the presence of Cl^-, NO_3^-, NO_2^-, SO_4^{2-}, and SO_3^{2-} anions at much greater levels than those toxic metals examined. The values of the standard free energy, enthalpy, and entropy proved that the sorption of As(V) and As(III) species onto the hybrid adsorbent TiO_2–SiO_2–PAN was an endothermic and spontaneous process. All of the results validated the feasibility of TiO_2–SiO_2–PAN for the highly effective removal of As(V) and As(III) from contaminated waters. © 2010 Wiley Periodicals, Inc. J Appl Polym Sci 119: 3495–3503, 2011

Key words: adsorption; amorphous; infrared spectroscopy; selectivity

INTRODUCTION

Arsenic is a widely distributed element in the earth's crust. Throughout the ages, arsenic has been used in medicine, cosmetics, agriculture, and industry. The occurrence of arsenic in ground water much exceeding the tolerance limit (0.01 mg/L) is a global problem and has posed an ever-increasing health hazard.[1] Arsenic intake from drinking water has been reported to increase the risk of cancer in the liver, lungs, skin, bladder, and kidneys.[2]

The distribution between arsenite [As(III)] and arsenate [As(V)] species in water depends on the redox potential and pH value.[3,4] As(III) is the predominant form of arsenic in underground water and is more toxic and mobile than As(V).[5] Because of the toxic nature of arsenic, the removal of trace arsenic from drinking water systems and industrial effluents has been of increasing importance. Several methods, namely, coagulation, adsorption, membrane filtration, and ion exchange are used to reduce the arsenic level below the tolerance value.[6–8] Among these techniques, adsorption has become increasingly popular during the last decade, and many articles have been published on the use of natural, synthetic, and surface-modified metal oxides, such as manganese, iron, aluminum, zirconium, tin, and titanium oxides, for the removal of arsenic from aqueous solutions.[9–18] Although inorganic metal oxides are effective in the removal of arsenic ions, a common drawback of oxides is that the spherical beads of suitable size for the required applications are usually very fine and difficult to obtain. To overcome this difficulty, hybrid sorbents were designed by the impregnation of these metal oxides onto conventional porous materials, namely, alginate, activated carbon, zeolite, diatomite, cellulose, and porous polymers. The host materials improved the permeability in flow-through systems without influencing the adsorption behaviors of the metal oxides, and thus, these resulting hybrid sorbents exhibited potential applications in heavy-metal retention.

More recently, porous polyacrylonitrile (PAN) polymers were used as more ideal alternatives to other host materials for inorganic adsorbent loading.[19–23] PAN beads are highly porous and can accommodate very high loadings of sorbents into the PAN matrix. These highly porous PAN beads exhibit a number of advantages over other granular

Correspondence to: A. Nilchi (anilchi@aeoi.org.ir).

sorbents. These advantages include significantly improved kinetics and sorbent capacity because of the increased availability of the sorbent material, easy modification of the physicochemical properties (hydrophilicity, porosity, and mechanical strength), and simplified production.

Hence, in this study, we focused on the loading of nanosized titania–silica binary oxide (TiO_2–SiO_2) binary oxide into the pores of the PAN polymer to prepare particles with higher granular strengths. Titania–silica mixed oxide is an interesting material for the adsorption of certain metal ions because the cation-exchange property of silica and the cation- and anion-exchange properties of titania are well known. The coprecipitation of titanium oxide and silica oxide seriously affects the surface properties (specific surface area, porosity, acidic sites, etc.) of each component; this provides a supplementary influence on the adsorption.[24,25] This article presents the preparative conditions, adsorption properties, and analytical applications of TiO_2–SiO_2–PAN polymeric–inorganic composite materials used as adsorbents for the removal of arsenic from aqueous solutions.

EXPERIMENTAL

Instruments

pH measurements were made with a Schott pH meter (model CG841) (Stafford, UK). The IR spectra were recorded with a Bruker Vector 22 spectrophotometer (Bruker, Germany). X-ray powder diffraction (XRD) was carried out with an 1800 PW Philips diffractometer (Nonius. B.V., Netherlands) with a Cu Kα beam to determine the structure of the adsorber. The X-ray source was a rotating anode operating at 40 kV and 30 mA with a copper target, and the data were collected between 2θ's of 20 and 80°. Thermogravimetric analysis (TGA) was carried out with a DuPont model 951 (Hartford, USA). The Brunauer–Emmett–Teller specific surface area and Barret–Joyner–Halenda pore size distribution of the sample were determined through nitrogen adsorption isotherms with a Quantachrome NOVA 2200e system (Hook, UK). Transmission electron micrographs were taken with a transmission electron microscope (Philips EM208S), and a scanning electron microscope (Philips XL30) was used to observe the pore structure and the distribution of TiO_2–SiO_2 powder in the beads. Finally, the amount of As was determined by a PerkinElmer (Buckinghamshire, UK) inductively coupled plasma (ICP) spectrometer (model 5500).

Materials

Titanium(IV) chloride (98%, Fluka, Buchs, Switzerland), tetraethylorthosilicate (98%, Merck, Bavaria, Germany), and ammonium hydroxide (25%, Fluka) were used as the starting materials without further purification. PAN was analytical grade and was obtained from Aldrich (Gillingham, England). Solutions were prepared in deionized water obtained with a Milli-Q water purification system (Buchs, Switzerland). Sodium arsenite ($NaAsO_2$) was used as the source of As(III) and was obtained from Fluka. The sodium salt of arsenic acid heptahydrate ($Na_2HAsO_4{\cdot}7H_2O$) was used as the source of As(V) and was obtained from Aldrich.

Adsorbent preparation

For TiO_2–SiO_2 preparation, $TiCl_4$ was added dropwise to deionized water under vigorous stirring in an ice water bath. The hydrolysis reaction was highly exothermic, and HCl was released. The produced dispersion was treated with NH_4OH, and the pH was adjusted to 7. The resulting solid was filtered and washed with deionized water to remove the chlorine ions. The precipitate was then dispersed in 200 mL of 0.3 mol/L HNO_3. The mixture was refluxed under vigorous stirring at 70°C for 16 h as titania sol was prepared. Tetraethylorthosilicate (25 mL) was added dropwise to the previous sol and stirred at 70°C. The resulting powder was filtered and washed with deionized water and then dried at room temperature. The prepared mixed oxide was calcined at 400°C for 1 h at a heating rate of 10°C/min.

To prepare the TiO_2–SiO_2–PAN beads; a weighed amount of TiO_2–SiO_2 binary mixed oxide powder was mixed with the solvent dimethyl sulfoxide and a few drops of Tween-80 surfactant and stirred at 50°C for 1 h. Then, 4.0 g of PAN powder was added to this solution with continuous stirring at 50°C for 2 h so that a homogeneous solution of the sorbent dope was obtained. The dissolved air in the dope was removed by a vacuum pump. The air-free composite dope was then passed inside the dual nozzle, the compressed air was ejected through the outside annulus of the dual nozzle, and hence, the size of the composite beads was adjusted accordingly.[26] The ejected composite beads were then dropped into a deionized water bath, which was used as a gelation agent. Finally, the beads were washed with demineralized water and dried at 50°C. They were then sieved in spherical beads with particle sizes from 1.0 to 2.0 mm.

Thermal and chemical stability

We carried out the thermogravimetric study by heating titania–silica oxide–PAN adsorber up to 800°C at a constant rate of 10°C/min in an argon atmosphere.

The chemical stabilities were determined by the placement of 0.1 g of the synthesized hybrid adsorber with 25 mL of different solvents for a period of 48 h at room temperature; this was followed

by the determination of the percentage of material that was dissolved.

Adsorption experiments

Aliquot portions of As(III) and As(V) were placed in 100 mL high-density polypropylene bottles after the adjustment of pH to the desired value with dilute sodium hydroxide or hydrochloric acid. TiO_2–SiO_2–PAN (0.1 g) was added to each of the test solutions, and the sample bottles were then placed in a thermostated shaker. At different time intervals, the supernatant solutions were filtered, and the concentration of arsenic were determined by inductively coupled plasma-atomic emission spectroscopy (ICP–AES). The effects of pH and temperature were then examined. The amount of arsenic ion adsorbed was expressed in terms of the distribution coefficient (K_d). K_d is defined as the concentration sorbed per gram of the sorbent divided by its concentration per milliliter at equilibrium. A higher K_d implies a higher selectivity or adsorption.

The investigation of the adsorption isotherm was conducted by a batch process. Arsenic solutions at different concentrations were prepared, and the pH values of these solutions were adjusted to the optimum value. TiO_2–SiO_2–PAN (0.1 g) was added to each sample. The samples were treated in a thermostatically controlled shaker at 25°C (298 K) for a specific period of contact time. The supernatant solutions were filtered, and the concentrations of the As(III) and As(V) ions were determined. The quantity of adsorbed arsenic on the synthesized adsorbent was calculated as the difference between the initial and final concentrations at equilibrium.

To evaluate the nature of adsorption, the experimental data were analyzed with the Freundlich, Langmuir, and Dubinin–Radushkevich (D–R) sorption models.

The Langmuir sorption isotherm has been widely used to characterize adsorption phenomena from solution. The isotherm is valid for monolayer adsorption onto a surface containing a finite number of identical sites. The form of the Langmuir isotherm can be represented by the following equation[27]:

$$\frac{C_e}{q_e} = \frac{1}{q_{\max} b} + \frac{C_e}{q_{\max}} \tag{1}$$

where C_e is the equilibrium concentration of ions remaining in the solution (mol/L), q_e is the amount of metal ions adsorbed per weight unit of the solid after equilibrium (mol/g), and $q_{\max}$ and b are Langmuir constants related to the sorption capacity and sorption energy, respectively. The maximum sorption capacity ($q_{\max}$) is the amount of adsorbate at complete monolayer coverage (mol/g) and b is a constant that relates to the heat of adsorption (L/mol).

The Freundlich isotherm model stipulates that the ratio of solute adsorbed to the solute concentration is a function of the solution. This model allows for several kinds of sorption sites on the solid and properly represents the sorption data at low and intermediate concentrations on heterogeneous surfaces.[28] The model has the following form:

$$\log q_e = \log K_F + n \log C_e \tag{2}$$

where k_F represents the sorption capacity when the metal-ion equilibrium concentration is equal to 1 [(mmol/g)(L/mmol)^n] and n represents the degree of dependence of sorption on the equilibrium concentration.

The D–R isotherm is more general than the Langmuir isotherm because it does not assume a homogeneous surface or a constant sorption potential. It is valid at low concentration ranges and can be used to describe sorption on homogeneous and heterogeneous surfaces. The D–R equation has the general expression[29]

$$\ln q_e = \ln q_{\max} - \beta\varepsilon^2 \tag{3}$$

where β is a constant related to the sorption energy (mol^2/kJ^2); ε is the Polanyi potential, which is equal to

$$\varepsilon = RT\ln(1 + 1/C) \tag{4}$$

where R is the ideal gas constant (8.3145 J mol^{-1} K^{-1}), C is equilibrium sorbate concentration (mg/L) and T is the absolute temperature (K). The saturation limit ($q_{\max}$) may represent the total specific micropore volume of the sorbent. The value of b is the activity coefficient related to the mean sorption energy (mol^2/kJ^2). It is related to the adsorption mean free energy [E (kJ/mol)], which is defined as the free energy change required to transfer 1 mol of ions from infinity in solution to the solid surfaces. The relation is as follows:

$$E = \frac{1}{\sqrt{2\beta}} \tag{5}$$

The magnitude of E is useful for estimating the type of sorption reaction. If E is in the range 8–16 kJ/mol, sorption is governed by chemical ion exchange. If E is less than 8 kJ/mol, physical forces may affect the sorption. On the other hand, sorption maybe dominated by particle diffusion if E is greater than 16 kJ/mol.[30]

RESULTS AND DISCUSSION

Characterization of the prepared sorbent

In this study, TiO_2–SiO_2 and its novel hybrid sorbent (TiO_2–SiO_2–PAN) were prepared. The resulting XRD

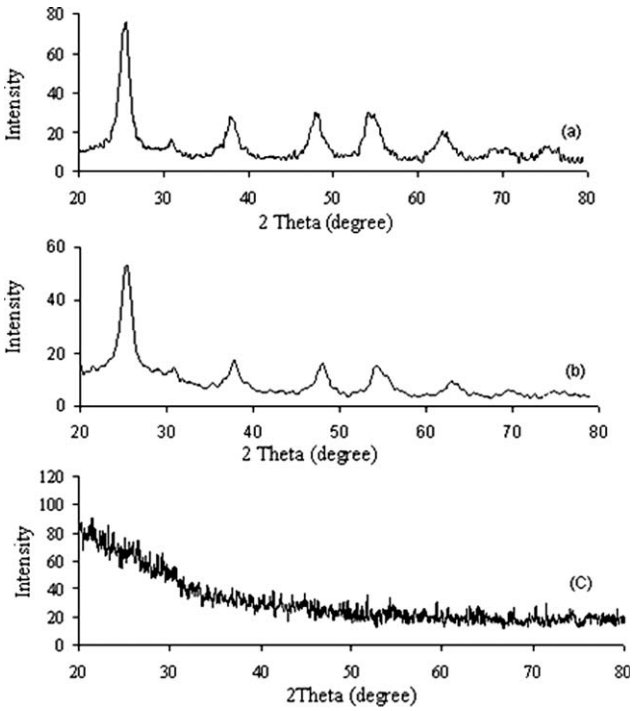

Figure 1 XRD patterns of (a) TiO_2–SiO_2 and (b) TiO_2–SiO_2–PAN.

patterns of TiO_2–SiO_2, TiO_2–SiO_2–PAN, and PAN are recorded in Figure 1. The XRD pattern of TiO_2–SiO_2 revealed that in addition to the brookite phase in the amorphous silica matrix, a crystalline anatase phase existed in TiO_2–SiO_2. The existence of brookite in the XRD pattern was clearly evidenced from the presence of the peak at $2\theta = 30.81°$. For the interpretation of the diffractograms, it was necessary to take into account that the main diffraction peak of anatase at $2\theta = 25.28°$ overlapped with the peaks of brookite at $2\theta = 25.34$ and $25.69°$, respectively.[31] We also observed that the 2θ values at the peak points of TiO_2–SiO_2–PAN were the same as those in TiO_2–SiO_2, and hence, their crystalline structure was very similar, but no diffraction peaks were observed for PAN; this indicated an amorphous structure. Furthermore, by comparing the XRD patterns, we determined that the synthesized TiO_2–SiO_2 binary oxide was loaded onto PAN.

The Fourier transform infrared spectra of the TiO_2–SiO_2 and TiO_2–SiO_2–PAN samples are shown in Figure 2. The band around 1100 cm^{-1} was the asymmetrical vibration of the Si—O—Si bond in the tetrahedral SiO_4 unit of the SiO_2 matrix. The absorption band at 954 cm^{-1} was ascribed to the vibration involving an SiO_4 tetrahedron bonded to a titanium atom through Si—O—Ti bonds. The presence of this band confirmed the presence of Si—O—Ti linkages in the synthesized product. The samples exhibited a band around 490 cm^{-1}, which was representative of TiO_2 matrices.[32] The broad band in the region 3200–3650 cm^{-1} was due to the stretching vibration of hydroxyl groups and interlayer water molecules, and the peak at 1620 cm^{-1} was assigned to the deformation vibration of the free water molecules. In the case of the composite, three characteristic bands were also observed at 2250, 1080, and 1453 cm^{-1}. A strong absorption peak at 2250 cm^{-1} was assigned to cyanide stretching vibrations. The spectrum of the sample showed the characteristic band for —CH_2 at 1453 cm^{-1}. The band at 1080 cm^{-1} was assigned to the overlapping of the stretching modes of C—O and Si—O—Si.

As shown in the transmission electron microscopy image of TiO_2–SiO_2, granular TiO_2 nanocrystallites (deep dark spots) were dispersed in the amorphous SiO_2 matrix [Fig. 3(a)].[33–35] The scanning electron microscopic photograph of the prepared TiO_2–SiO_2–PAN sorbent bead is shown in Figure 3(b). The results reveal that the particles were not homogeneous. The pore size of the inner part of the particles was larger than those near the surface. The kinetics of sorption on these adsorber beads must have been very fast because the TiO_2–SiO_2 powder, which was the active material, was dispersed throughout the binding matrix.

Numerical data of the nitrogen adsorption isotherm for the synthesized TiO_2–SiO_2–PAN revealed that the prepared material had a Brunauer–Emmett–Teller surface area of 170 m^2/g, and according to a Barret–Joyner–Halenda plot, the pore diameter of TiO_2–SiO_2–PAN was 2.89 nm. However, the surface area and pore size of PAN were found to be 248 m^2/g and 2.92 nm, respectively. This showed that the surface area and pore diameter of the hybrid adsorbent was much lower than that of PAN.

The thermogravimetric curve of synthesized TiO_2–SiO_2–PAN is shown in Figure 4. The curve indicates that the weight decrease that was caused by the vaporization of physisorbed water continued until about 250°C. Then, between 250 and 300°C, the PAN

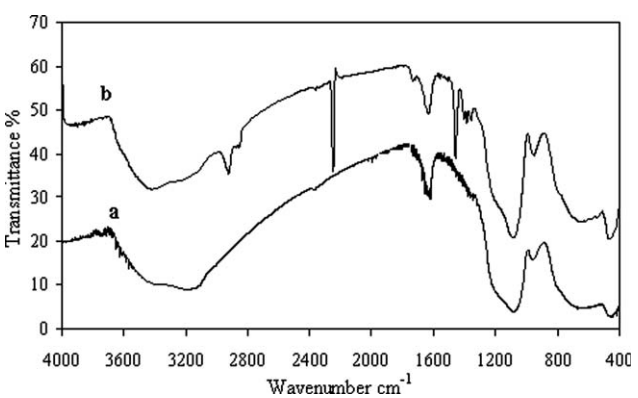

Figure 2 Fourier transform infrared spectra of (a) TiO_2–SiO_2 and (b) TiO_2–SiO_2–PAN.

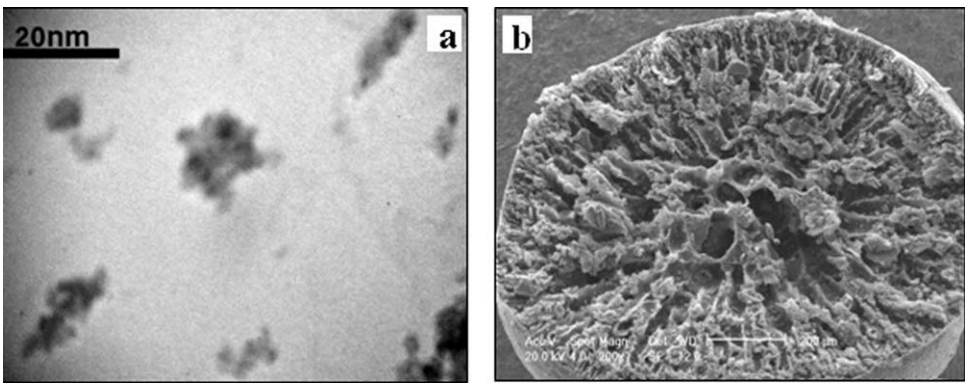

Figure 3 (a) Transmission electron microscopy image of the synthesized TiO_2–SiO_2 and (b) scanning electron micrograph of the TiO_2–SiO_2–PAN adsorber bead cross section.

fiber was first stretched and simultaneously oxidized. This treatment converted thermoplastic PAN to a nonplastic cyclic or a ladder compound. The decrease of oxygen as water vapor was due to the evolution of H_2O in the region 300–400°C. The evolution of H_2O was caused by the crosslinking condensation reactions between the two monomer units of the adjacent ladder polymeric molecular chains. The decrease in weight around 400°C was the result of the small portion of anatase crystallizing to brookite. As the temperature increased up to 800°C, hydrogen cyanide and ammonia gases were also released with water.[36] The analysis of the TGA curve clearly showed that TiO_2–SiO_2–PAN in granule form was thermally stable up to 250°C.

TiO_2–SiO_2–PAN was found to be stable in water, dilute mineral acids, ethanol, methanol, acetone, and ether. However, in dimethyl sulfoxide, concentrated HCl, 5 mol/L H_2SO_4, 8 mol/L HNO_3, and 5 mol/L H_3PO_4, it decomposed. The synthesized adsorbent was stable in all common aqueous electrolytes, except in concentrated solutions of $ZrCl_2$, LiBr, $CaCl_2$, and NaSCN, which are known to dissolve PAN.

Effect of pH on the arsenic adsorption

pH is an important parameter influencing metal-ion adsorption from aqueous solutions. Figure 5 represents the effect of the initial pH of the solution on the K_d values of the As(V) and As(III) ions. The results show that the K_d values of As(III) were lower in the acidic region but higher from the neutral to the alkaline region, whereas for As(V), K_d was higher in the acidic range. As(V) species can exist in an aqueous solution as oxo-anions because the pK_{a1} and pK_{a2} values of H_3AsO_4 are 2.24 and 6.96, respectively,[34] and the predominant As(V) species adsorbed should be $H_2AsO_4^-$. The data for As(III) suggest that nonionic H_3AsO_3 is likely to be responsible for the adsorption because the pK_{a1} value of H_3AsO_3 is 9.1.[37] In this study, a pH of 6 for As(V) and a pH of 8 for As(III) were chosen for further adsorption studies.

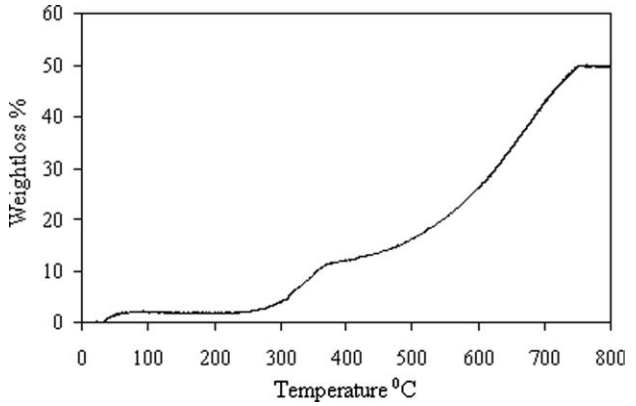

Figure 4 TGA curve of the TiO_2–SiO_2-loaded PAN polymer.

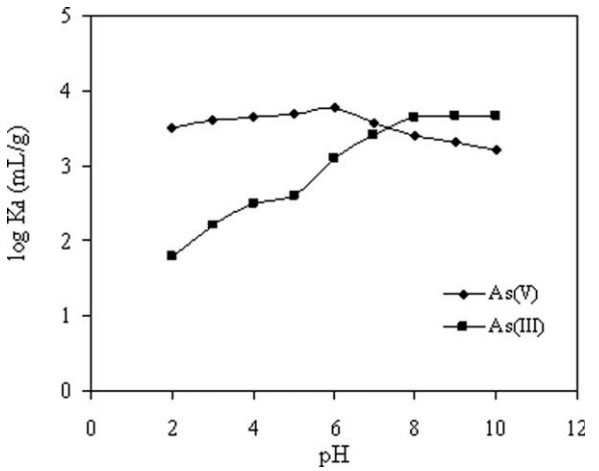

Figure 5 Effect of the pH on K_d of the As(III) and As(V) ions.

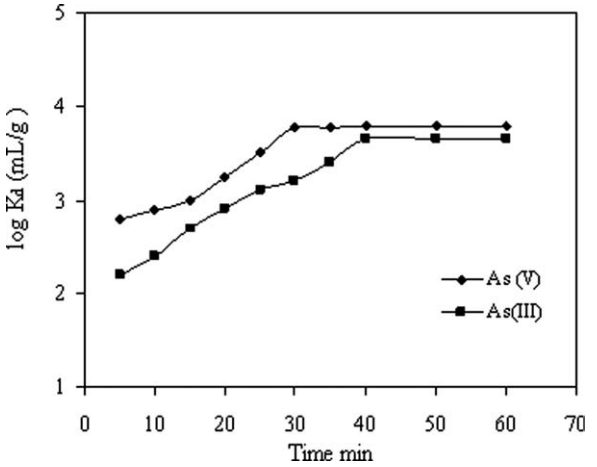

Figure 6 Effect of the contact time on K_d of the As(III) and As(V) ions.

Effect of the contact time

Figure 6 shows the effect of the contact time on the K_d values of As(III) and As(V) for the prepared hybrid adsorbent. Figure 6 clearly shows that the K_d values of As(V) increased with increasing contact time and attained equilibrium in about 30 min. The adsorption of As(III) increased with increasing contact time and reached a maximum value after 40 min; hence, a contact time of 60 min was chosen for further studies.

Effect of the diverse ions

The efficiency of the sorbent for the removal of arsenic in the treatment of industrial or natural water is affected by its selectivity in various common chemical species. The influence of coexisting ions (10^{-3} mol/L) toward the adsorption of As(III) and As(V) (10^{-4} mol/L, respectively) was examined, as shown in Table I.

TABLE I
Effect of the Added Ions on K_d of the Arsenic Ions on TiO_2–SiO_2–PAN

	K_d (mL/g)	
Added ion	AS(III)	AS(V)
Nil	4467	5888
PO_4^{3-}	1438	2512
Cl^-	4421	5846
NO_3^-	4457	5814
NO_2^-	4460	5879
SO_4^-	4395	5873
SO_3^{2-}	4411	5756
Cd(II)	4450	5843
Na(I)	4399	5776
Pb(II)	4418	5830
Fe(III)	2118	3649
Co(II)	2205	3517
Cu(II)	2968	5668
Cr(VI)	2900	5722

Conditions: temperature = 298 K; pH = 6 for As(V) and pH = 8 for As(III).

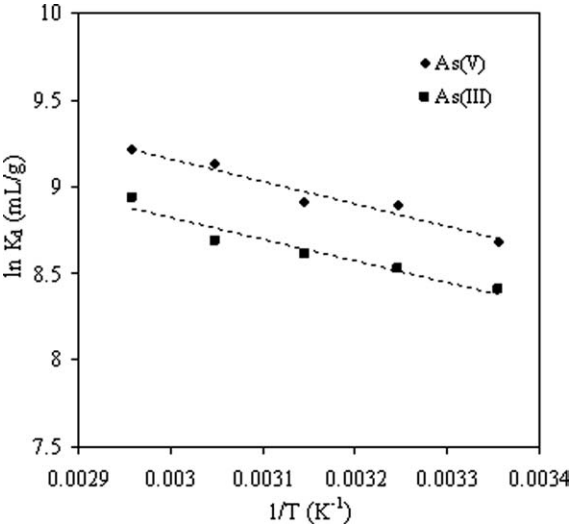

Figure 7 Effect of the temperature on K_d of As(III) and As(V).

The adsorption of arsenic was not affected by the presence of anions such as Cl^-, NO_3^-, NO_2^-, SO_4^{2-}, and SO_3^{2-}. However, PO_4^{3-} ions interfered with the adsorption of both As(III) and As(V), most significantly because of the mutual similarity of the ions with respect to their chemical form and the pK_a value.[37]

The presence of cations, such as Cd(II), Na(I), and Pb(II), even in large excess, had no significant effect on the arsenic adsorption. However, Fe(III) and Co(II) interfered with the adsorption of both As(III) and As(V), whereas Cu(II) and Cr(VI) only affected As(III).

Adsorption thermodynamics

The thermodynamic parameters, the values of standard free energy or Gibbs free energy change (ΔG°),

TABLE II
Thermodynamic Parameters for Arsenic Adsorption onto TiO_2–SiO_2–PAN

Species	Temperature (°C)	$-\Delta G^\circ$ (kJ/mol)	ΔH° (kJ/mol)	ΔS° (kJ mol^{-1} K^{-1})
As(V)	298	21.487	10.849	0.108
	308	22.415		
	318	23.495		
	328	24.575		
	338	25.655		
As(III)	298	20.789	10.449	0.105
	308	21.838		
	318	22.886		
	328	23.934		
	338	24.983		

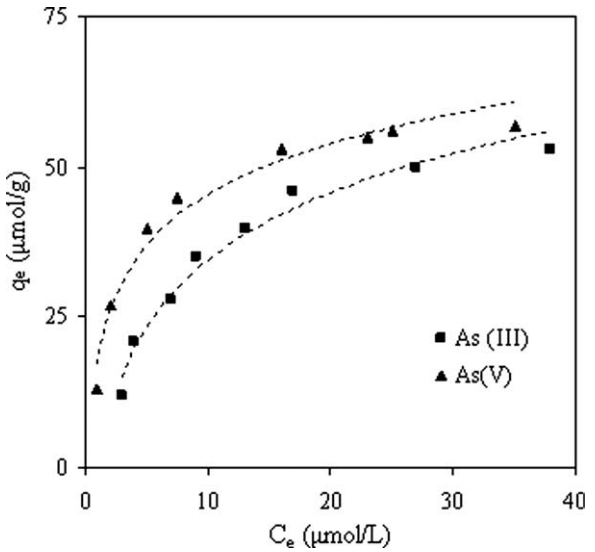

Figure 8 Sorption isotherms of As(V) and As(III) on TiO_2–SiO_2–PAN.

standard enthalpy (ΔH°), and standard entropy (ΔS°) of the sorption, were useful in defining whether the sorption reaction was endothermic or exothermic and for defining the spontaneity of the adsorption process. The parameters were calculated with the following equations:

$$\ln K_d = \frac{-\Delta H^\circ}{RT} + \frac{\Delta S^\circ}{R} \quad (6)$$

$$\Delta G = \Delta H - T\Delta S \quad (7)$$

The values of ΔH° and ΔS° were obtained from the slope and intercept of the linear variation of ln K_d with reciprocal temperature (Fig. 7). The relevant data calculated from the previous equations are tabulated in Table II.

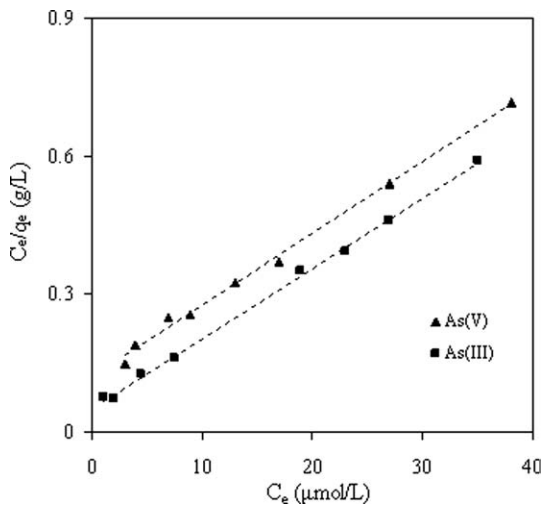

Figure 9 Langmuir adsorption isotherms of As(III) and As(V).

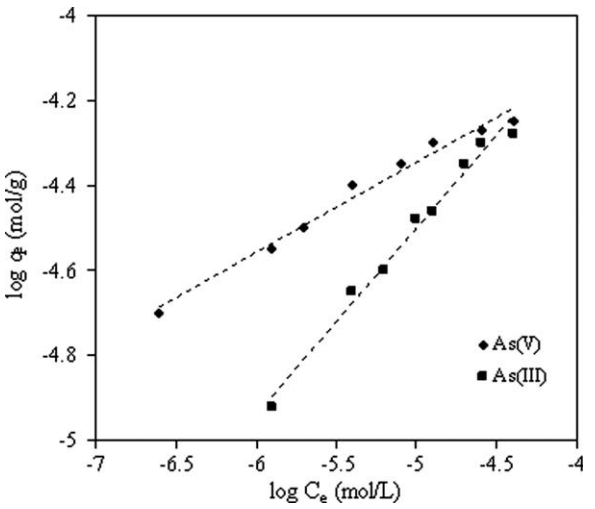

Figure 10 Freundlich adsorption isotherms of As(III) and As(V).

The adsorption of As(V) and As(III) increased with increasing temperature, and the value of ΔH° was positive. The positive ΔH° value confirmed that the adsorption process was endothermic for arsenic; this was an indication of the existence of a strong interaction between the adsorbent and the As(V) and As(III) ions. ΔG° was negative as expected for a spontaneous process under the conditions applied. The positive values of ΔS° reflected the affinity of TiO_2–SiO_2–PAN toward arsenic ions in aqueous solutions and may suggest some structural changes in the adsorbent.

Sorption isotherms

The equilibrium data of arsenic adsorption by the TiO_2–SiO_2–PAN obtained at 25°C (298 K) are shown as points in Figure 8.

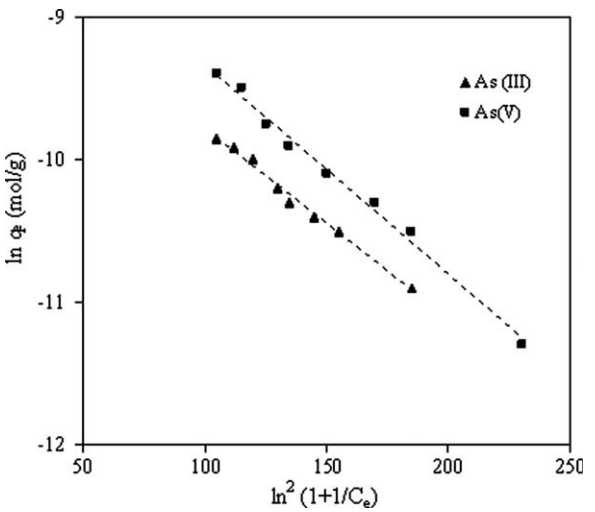

Figure 11 D–R adsorption isotherms of As(III) and As(V).

TABLE III
Isotherm Parameters Obtained from the Analysis of the Arsenic Adsorption

Isotherm model	Estimated isotherm parameter					
	As(III)			As(V)		
Langmuir	$b = 1.52 \times 10^5$ L/mol	$q_{max} = 6.53 \times 10^{-5}$ mol/g	$R^2 = 0.99$	$b = 4.58 \times 10^4$ L/mol	$q_{max} = 6.99 \times 10^{-5}$ mol/g	$R^2 = 0.99$
Freundlich	$K_F = 0.6 \times 10^{-2}$ (mol/g)(L/mol)^n	$n = 0.45$	$R^2 = 0.98$	$K_F = 0.2 \times 10^{-2}$ (mol/g)(L/mol)^n	$n = 0.30$	$R^2 = 0.98$
D–R	$\beta = 2.90 \times 10^{-3}$ mol^2/kJ^2	$q_{max} = 4.72 \times 10^{-4}$ mol/g	$E = 13.1$ kJ/mol $R^2 = 0.99$	$\beta = 3.74 \times 10^{-3}$ mol^2/kJ^2	$q_{max} = 7.84 \times 10^{-4}$ mol/g	$E = 11.6$ kJ/mol $R^2 = 0.99$

The Freundlich, Langmuir, and D–R sorption isotherms of arsenic are shown in Figures 9–11, respectively. The relative parameters and the correlation coefficients calculated from eqs. (1)–(5) are listed in Table III. The correlation coefficients indicated that the sorption was fitted by the Langmuir and D–R models better than by the Freundlich model.

Total sorption capacity

TiO_2–SiO_2–PAN beads (0.1 g) were stirred for 5 h with 100 mL of a 0.1 mol/L solution of As(V) and As(III) at optimum pH. The metal-ion concentration in the supernatant liquid was estimated by ICP–AES. The sorption capacity of the prepared sorbent for each ion was ascertained from the difference between the metal-ion concentration in solution before and after sorption. The adsorption capacity of the adsorbent was found to be 0.47 mmol/g of adsorber for As(V) and 0.39 mmol/g for As(III).

Stability and reusability of the resin

Arsenic was sorbed and desorbed on 1 g of the TiO_2–SiO_2–PAN repeatedly. The sorption capacity of adsorbent after five cycles of its equilibration with arsenic changed by less than 11%. Therefore, repeated use of the synthesized sorbent was feasible. The adsorber could be regenerated with 1 mol/L H_2SO_4.

CONCLUSIONS

The polymer-supported TiO_2–SiO_2 prepared in this study was an extremely effective adsorbent for arsenic retention from water. Arsenic adsorption onto TiO_2–SiO_2–PAN was pH dependent. Also, the prepared adsorbent exhibited more favorable arsenic adsorption in the presence of other competing anions, such as Cl^-, NO_3^-, NO_2^-, SO_4^{2-}, and SO_3^{2-}, with the exception of PO_4^3. The adsorption of As(III) and As(V) by the hybrid adsorbent was found to be an endothermic and spontaneous process. Furthermore, the results indicate that the arsenic sorption could be fitted by the Langmuir and D–R models better than the Freundlich one. Moreover, the exhausted TiO_2–SiO_2–PAN beads were amenable to efficient regeneration by a 1 mol/L H_2SO_4 solution for repeated use without any significant capacity loss.

References

1. Smedley, P. L.; Kinniburgh, G. Appl Geochem 2002, 17, 517.
2. Wang, J. P.; Qi, L.; Moore, M. R.; Ng, J. C. Toxicol Lett 2002, 133, 17.
3. Cullen, W. R.; Reimer, K. J. Chem Rev 1989, 89, 713.
4. Masscheleyn, P. H.; Delaune, R. D.; Patrick, W. H. Environ Sci Technol 1991, 25, 1414.
5. Wang, J. S.; Wai, C. M. J Chem Educ 2004, 81, 207.

6. Hering, J. G.; Chen, P.; Wilkie, J. A.; Elimelech, M. J Environ Eng ASCE 1997, 123, 800.
7. Kartinen, E. O.; Martin, C. J. J Desal 1995, 103, 79.
8. Nikolaidis, N. P.; Dobbs, G. M.; Lackovic, J. A. Water Res 2003, 37, 1417.
9. Lin, T. F.; Wu, J. K. Water Res 2001, 35, 2049.
10. Gupta, K.; Ghosh, U. C. J Hazard Mater 2009, 161, 884.
11. Manna, B. R.; Ghosh, U. C. J Hazard Mater 2007, 144, 522.
12. Bajpai, S.; Chaudhuri, M. J Environ Eng 1999, 125, 782.
13. Manna, B. R.; Debnath, S.; Hossain, J.; Ghosh, U. C. J Ind Pollut Control 2004, 20, 247.
14. Grossl, P. R.; Eick, M.; Sparks, D. L.; Goldberg, S.; Ainsworth, C. C. Environ Sci Technol 1997, 31, 321.
15. Kundu, S.; Gupta, K. J Hazard. Mater 2007, 142, 97.
16. White, D. A.; Rautiu, R. Chem Eng J 1997, 66, 85.
17. Dutta, P. K.; Ray, A. K.; Sharma, V. K.; Millero, F. J. J Colloid Interface Sci 2004, 278, 270.
18. Bang, S.; Patel, M.; Lippincott, L.; Meng, X. Chemosphere 2005, 60, 389.
19. Ali, I. M.; El-Zahhar, A. A.; Zakaria, E. S. J Radioanal Nucl Chem 2005, 264, 637.
20. Kim, H. T.; Lee, C. H.; Shul, Y. G.; Moon, J. K.; Lee, E. H. Sep Sci Technol 2003, 38, 695.
21. Nilchi, A.; Khanchi, A.; Atashi, H.; Bagheri, A.; Nematollahi, L. J Hazard Mater 2006, 137, 1271.
22. Šebesta, F. J Radioanal Nucl Chem 1997, 220, 77.
23. Someda, H. H.; El Zahhar, A. A.; Shehata, M. K.; El-Naggar, H. A. Sep Purif Technol 2002, 29, 53.
24. Iler, R. K. The Chemistry of Silica; Wiley: New York, 1978.
25. Venkataramani, B. In New Developments in Ion Exchange: Proceeding of International Conference on Ion Exchange, ICIE'91, Tokyo, Japan; Abe, M.; Kataoka, T.; Suzuki, T., Eds.; Elsevier: Amsterdam, 1991.
26. Moon, J. K.; Kim, K. W.; Jung, C. H.; Shul, Y. G.; Lee, E. H. J Radioanal Nucl Chem 2000, 246, 299.
27. Langmuir, I. J Am Chem Soc 1916, 38, 2221.
28. Freundlich, H. Phys Chem A 1906, 57, 385.
29. Dubinin, M. M. Chem Rev 1960, 60, 235.
30. Tan, X. L.; Wang, X. K.; Fang, M.; Chen, C. L. Colloids Surf A 2007, 296, 109.
31. Paola, A.; Cufalo, G.; Addamo, M.; Bellardita, M.; Campostrini, R.; Ischia, M.; Ceccato, R.; Palmisano, L. J Colloid Interface Sci A 2008, 317, 366.
32. Amlouk, A.; Mir, L. E.; Kraiem, S.; Alaya, S. J. Phys Chem Solid 2006, 67, 1464.
33. Raveendran, P.; Eswaramoorthy, M.; Bindu, U.; Chatterjee, M.; Hakuta, Y; Kawanami, H.; Mizukami, F. J Phys Chem C 2008, 112, 20007.
34. Ao, Y.; Xu, J.; Fu, D.; Yuan, C. Mesopor Mater 2009, 122, 1.
35. Wang, G, J. Mol Catal A 2007, 274, 185.
36. Rahaman, M. S. A.; Ismail, A. F.; Mustafa, A. Polym Degrad Stab 2007, 92, 1421.
37. Martell, A. E.; Smith, R. M. Critical Stability Constants; Plenum: New York, 1979.